Int. J. Electrochem. Sci., 5 (**2010**) 344 - 354

International Journal of
ELECTROCHEMICAL
SCIENCE
www.electrochemsci.org

Formic Acid Oxidation at Pd, Pt and PbO_x-based Catalysts and Calculation of their Approximate Electrochemical Active Areas

Rafael V. Niquirilo, Erico Teixeira-Neto, Guilherme S. Buzzo and Hugo B. Suffredini[*]

Universidade Federal do ABC, Centro de Ciências Naturais e Humanas,
Rua Santa Adélia 166, Bairro Bangu, Santo André, SP, Brazil
[*]E-mail: hugo.suffredini@ufabc.edu.br

Received: 23 January 2010 / *Accepted:* 15 March 2010 / *Published:* 31 March 2010

In this work, we describe the use of several Pd-based catalysts for promotion of the oxidation of formic acid in the presence of sulphuric acid. We also undertake and discuss a calculation of the "electrochemical area" of the carbon-supported catalysts, by using a polycrystalline Pt electrode and a $Fe(CN)_6^{3-}/Fe(CN)_6^{4-}$ solution. All catalysts were synthesized by a modified sol-gel method. XRD spectra revealed that the Pd/C catalyst particles were a mixture of Pd and PdO crystallites. Particles of the Pd-Pt/C catalyst were composed mainly of a mixture of Pd, Pt or PdPt crystallites. The Pd-Pt-PbO_x/C particles were a mixture of crystallites of Pd, Pt (or PdPt), PdO and lead oxides. Examination of their electrochemical responses showed that the Pd-Pt-PbO_x/C catalysts are well suited to promote formic acid oxidation, as they avoid strong ion adsorption processes on the electrode surfaces, a problem commonly observed when using Pd/C catalysts.

Keywords: Palladium-based Catalysts; Lead Oxides; Formic Acid Oxidation; Electrochemical Area.

1. INTRODUCTION

Palladium-based materials are state-of-the-art catalysts for promoting the oxidation of formic acid in electrochemical devices. In this context, several groups around the world are studying the mechanisms of oxidation [1-5] and the catalytic properties of Pd-carbon-supported materials [6-11]. Mainly, they aim to use these kinds of catalysts as anodes in direct formic acid fuel cells (DFAFC). Pd and Pd alloys have been studied in the literature with interesting results. For example, Waszczuk et al. [12] synthesized nanoparticles containing Pd, Ru and Pt. The Pt-Pd catalyst performed best, and the authors suggested that direct CO_2 formation on Pt-Pd is much less affected by the CO chemisorption than on pure Pt or on a Pt-Pd-Ru catalyst.

One of the most accepted mechanisms of formic acid oxidation are described below. The first mechanism, called "direct pathway," involves direct oxidation of the acid to carbon dioxide:

$$HCOOH + Me \rightarrow CO_2 + 2H^+ + Me + 2e^- \qquad \text{(eq. 1)}$$
("Me" = Pt, Pd and other)

A second mechanism occurs when carbon monoxide adsorbs onto a "Me" surface, and two electrochemical steps follow:

$$HCOOH + Me \rightarrow Me\text{-}CO + H_2O \qquad \text{(eq. 2)}$$
$$Me + H_2O \rightarrow Me\text{-}OH + H^+ + e^- \qquad \text{(eq. 3)}$$
$$Me\text{-}CO + Me\text{-}OH \rightarrow 2Me + CO_2 + H^+ + e^- \qquad \text{(eq. 4)}$$

It is well established that Pd promotes the "direct pathway" mechanism of formic acid oxidation (eq. 1). On the other hand, slow and continuous decay is commonly observed in current vs. time experiments of oxidation of this acid in several media when Pd is used as anode. This effect is most likely related to the presence of other poisoning agents, such as formate [13], sulphate [14] and other anions [15]. On the other hand, a Pt electrode promotes the indirect mechanism (eqs. 2, 3 and 4). These effects were discussed in a communication published by Yu and Pickup [16].

The determination of real electroactive areas for carbon-supported catalysts is not an easy task. Several experimental techniques are commonly used to make this determination, including stripping of adsorbed carbon monoxide charge [17], normalizing by catalyst mass [18] and determining the hydrogen charge related to the desorption of hydrogen on the electrode surface [19]. Normalization of currents by CO desorption is not the best choice for several materials, including Pd, simply because these do not have an affinity for carbon monoxide. Normalization of currents by catalyst mass (with A/gPt, for example) is also questionable in several cases. This is mainly due to the dynamic properties of the material when a second or a third metal is present. Finally, determination of real areas for some bimetallic materials using the hydrogen desorption technique is not interesting because the Hydrogen-UPD signal is inhibited by the presence of this second metal.

One possible technique for approximating the electrochemical area of a catalyst involves using a polycrystalline Pt electrode and a $Fe(CN)_6^{3-}/Fe(CN)_6^{4-}$ solution as references. This "electrochemical area" is related to the current detected by the potentiostat in the electrochemical experiment. This technique is described in further detail in the experimental section and discussed in the results chapter of this paper.

Some publications demonstrate that the presence of metallic Pb or lead oxides can improve the catalytic performance of noble metals, such as platinum. In this way, Abruña and co-authors discussed the use of Pb or Bi-based electrodes to oxidize several organic molecules, demonstrating that the catalytic performance is superior when these metals are used as *co*-catalysts [20-22].

Similarly, Suffredini et al. [23, 24] published two papers respectively concerning methanol and ethanol oxidation, showing that the presence of lead oxides drastically increased the catalytic activity of the anodes. In these studies, the lead-based catalysts were described as being "PbO_x" (a mixture of PbO and PbO_2) and the platinum was polycrystalline Pt, constituting separated crystallographic phases.

These materials were prepared by an adaptation of the traditional sol-gel method, which is largely used to synthesize materials such as supercapacitors [25], diodes [26] or catalysts [27]. The adapted sol-gel method is a feasible and easy way to synthesize this kind of material.

Thus, the first aim of this work is to investigate the performance of Pd, Pt and PbO_x-based catalysts using electrochemical methods such as cyclic voltammetry and current-time measurements. The second aim is to calculate the approximate electrochemical areas of all catalysts using a polycrystalline Pt electrode and a $Fe(CN)_6^{3-}/Fe(CN)_6^{4-}$ solution as references.

2. EXPERIMENTAL PART

2.1. XRD spectra

The crystalline structures of the investigated catalysts were determined using techniques of powder X-ray diffraction. Data were recorded in a Rigaku diffractometer (Miniflex model) using a Cu-Kα radiation source (1.5406 Å, 30 kV and 15 mA). About 30 mg of each powdered sample was kept in a glass sample holder and pressed using a glass slide to obtain a uniform distribution. The 2θ Bragg angles were scanned over a range of 20–85° at a rate of 2° per minute with a 0.02° angular resolution.

2.2. Working electrode preparation

All catalysts were prepared using an adapted sol-gel method, as described in detail in previous work [23, 24]. Basically, appropriate quantities of acetylacetonates of Pd, Pt or Pb (or mixtures of the three organic compounds), prepared in a mixture of ethanol and acetic acid (3:2, v/v), were added to 0.20 g of carbon powder (Vulcan® XC72R), to achieve a catalyst load of approximately 10 % (by mass, with respect to the carbon powder). Modified powders were treated for 1 hour at a temperature of 400 ^{o}C for 60 minutes, under a nitrogen atmosphere.

0.008 g of each of the modified powders were added to a mixture containing 1000 μL of water + 40 μL of a 5% Nafion® solution (5% in aliphatic alcohols). These mixtures were then transferred to an ultrasonic bath (for 5 minutes), to produce black inks. Then, 5 μL of the inks were transferred to a glassy carbon electrode (geometric area of 0.031 cm^2), previously polished with alumina and washed with isopropyl alcohol.

2.3. Electrochemical Experiments

Cyclic voltammetry, chronoamperometry and calculation of electrochemical areas were carried out using an Autolab PGSTAT 100 potentiostat/galvanostat. A one-compartment electrochemical cell was used for al measurements. The working electrode was glassy carbon (modified with carbon powder), the auxiliary electrode was a Pt foil with a 2 cm^2 geometric area and the reference electrode was Ag/AgCl (KCl saturated). The supporting electrolyte was a H_2SO_4 0.5 mol L^{-1} solution (Merck®) also containing, in some cases, formic acid at a concentration of 1.0 mol L^{-1} (Synth®)

Calculations of approximate electrochemical areas were carried out using the protocol described below.

1) The real area of a selected polycrystalline Pt electrode (1.1 cm^2 of geometric area) was determined by studying H-desorption in the presence of sulphuric acid (0.5 mol L^{-1} supra pure H_2SO_4), after saturating the cell with ultrapure N_2. For a polycrystalline Pt electrode, it is known that an average charge of 210 μC is associated with the desorption of hydrogen for each 1 cm^2 of exposed Pt surface in acidic solution. Thus, measurement of the H-desorption charge can determine the real area of a polycrystalline Pt electrode.

2) After the real area of a selected Pt electrode is determined, cyclic voltammetry is performed on a well-known reversible electrochemical reaction in solution. Here we use a $Fe(CN)_6^{3-}/Fe(CN)_6^{4-}$ redox pair. This generates a voltammogram of the Pt electrode in the redox pair-containing solution. Solutions consisted of 1.0 mol L^{-1} $Fe(CN)_6^{3-}/Fe(CN)_6^{4-}$, prepared in a 0.5 mol L^{-1} H_2SO_4 support electrolyte. Despite its high stability, related to the effect of ligand, potassium ferro/ferricyanide can decompose in acid media if the temperature of operation is high. Preparation and handling of this solution should be held in the fume hood, also using masks and gloves.

3) Finally, the test materials – those for which the approximate electrochemical area is to be determined – are subject to the procedure described in step 2. The test materials in this paper include Pt, Pb and Pd-based catalysts supported in carbon powder. A comparison can then be drawn between the peak currents of the Pt electrode and those of the unknown material.

3. RESULTS AND DISCUSSION

3.1. XRD spectra

X-ray diffraction patterns for Pd/C, Pd-Pt/C and Pd-Pt-PbO_x/C catalysts are presented in Figure 1, and they reveal the metallic phases present within the materials.

The broad reflections observed at $2\theta = 25°$ in all patterns is due to the (002) reflection from the carbon support. The characteristic reflections from the face centred cubic (fcc) structures of both Pd and Pt are also present where expected, as identified by the ICDD Powder Diffraction Files (ICDD-PDF). Within this 2θ range, reflections from the fcc planes (111), (200), (220) and (311), at respectively 40°, 46°, 68° and 82°, are seen in the XRD patterns of all materials. This indicates the presence of Pd metallic crystallites within the Pd/C material and reveals the presence of a mixture of Pd, Pt and PdPt alloyed crystallites within the Pd-Pt/C and Pd-Pt-PbO_x/C materials. XRD reflections obtained from PdO crystallites (ICDD-PDF), as indicated by the arrows in the Pd-Pt/C pattern, are also present in all materials. Comparing the patterns of the different catalysts, the Pd-Pt/C electrodes had smaller relative PdO peaks, revealing a smaller proportion of PdO crystallites within its structure.

Additional peaks observed in the Pd-Pt-PbO_x/C material were identified (ICDD-PDF) as mixtures of different Pb oxides.

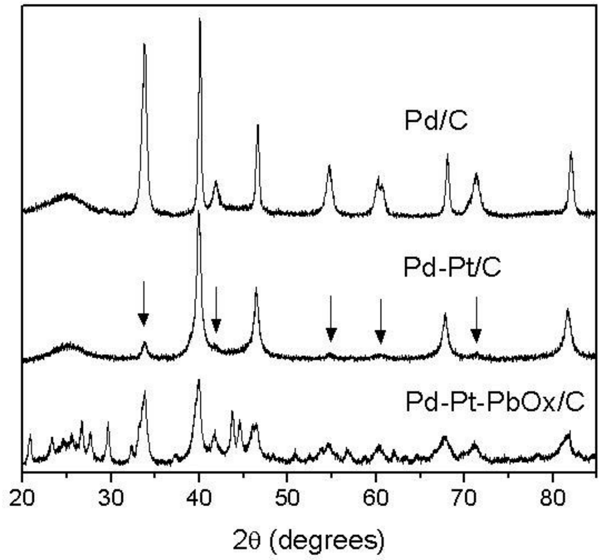

Figure 1. X-ray diffraction patterns for Pd/C, Pd-Pt/C and Pd-Pt-PbO_x/C catalysts. PdO reflections are indicated by arrows in the Pd-Pt/C pattern. Among the catalysts, Pd-Pt/C has a smaller relative proportion of PdO crystallites within its structure.

3.2. Approximate electrochemical active area calculation

Figure 2 shows the results from electrochemical experiments carried out to determine the electrochemical areas of catalysts Pd/C, Pd-Pt/C and Pd-Pt-PbO_x/C. It is possible to determine the approximate electrochemical area of an electrode by comparing the currents of oxidation (or reduction, for a reversible pair) of the $Fe(CN)_6^{3-}/Fe(CN)_6^{4-}$ redox couple in acidic solution, following the relationship (eq. 5):

$$A(elet.)_{UM} = \frac{\Delta I_{(UM)}.A(elet.)_{Pt}}{\Delta I_{(Pt)}} \quad \text{(eq. 5)}$$

where $A(elet.)_{UM}$ and $\Delta I_{(UM)}$ are the electrochemical area and the peak current of oxidation, respectively, for the unknown material. $A(elet.)_{Pt}$ and $\Delta I_{(Pt)}$ represent the real area and the peak current of oxidation for a polycrystalline Pt control electrode with well-established real area. This real area was calculated by determining the charge affiliated with hydrogen desorption on the polycrystalline Pt plate. The inset of Figure 2(a) shows the response of the polycrystalline Pt electrode to ultrapure H_2SO_4 at a concentration of 0.5 mol L^{-1}, as measured over several scan rates. The mean value of the hydrogen desorption charge was 8.83 x 10^{-4} C, corresponding to a real area of 4.2 cm^2. The geometric area of the Pt working electrode was 1.1 cm^2. Thus, the roughness factor for this electrode was 3.82. The arrow between the inset and the cyclic voltammogram (CV) in Fig. 2(a) shows that the CV depended particularly on the measurements presented in the inset.

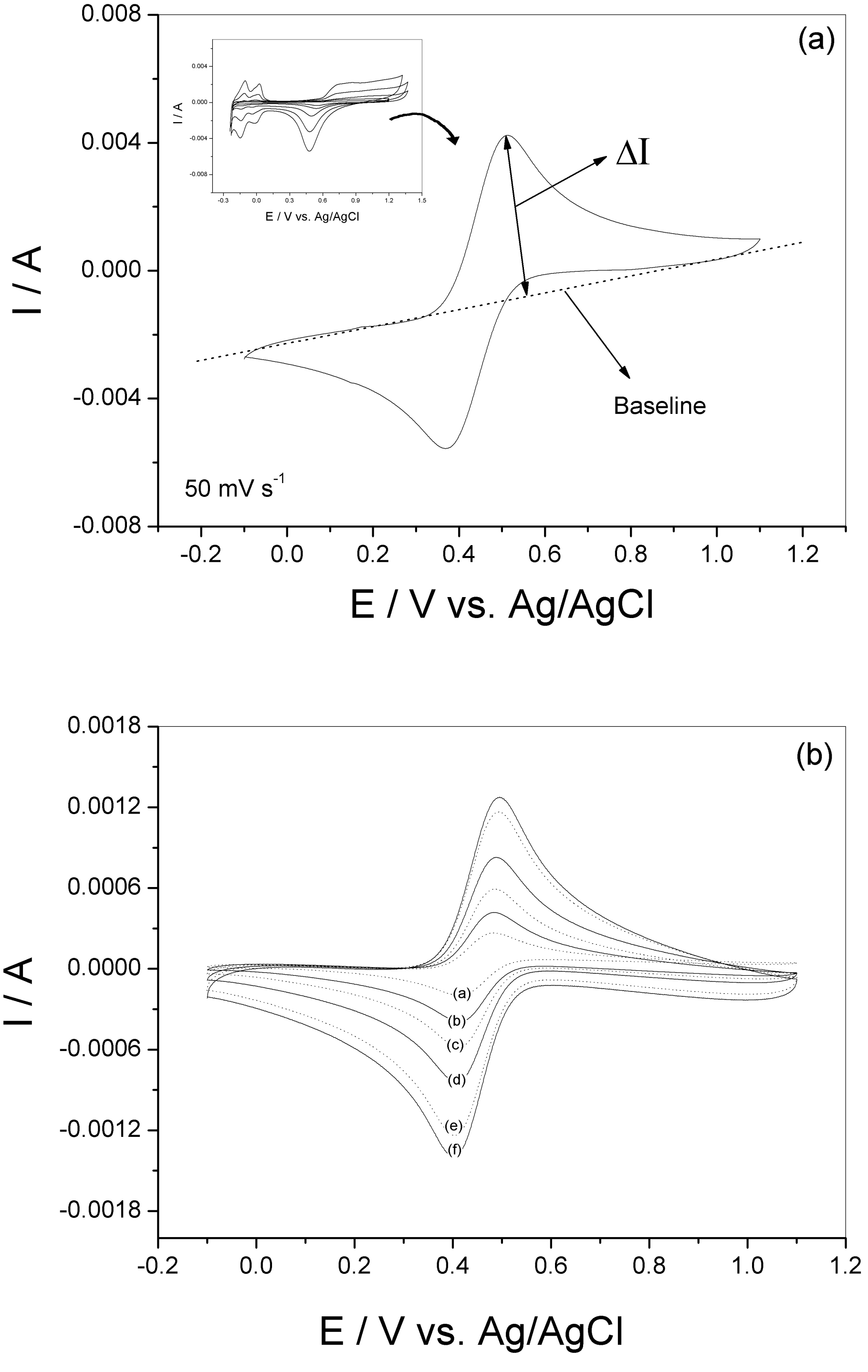

Figure 2. Calculation of the approximate "electrochemical active areas" for Pd/C, Pd-Pt/C and Pd-Pt-PbO_x/C catalysts. Figure 2(a) represents the electrochemical response of a polycrystalline Pt electrode in a 1.0 mol L^{-1} $Fe(CN)_6^{3-}/Fe(CN)_6^{4-}$ + 0.5 mol L^{-1} H_2SO_4 solution, obtained at a scan rate of 50 mV s^{-1}. The insets present the response of a Pt catalyst in a 0.5 mol L^{-1} H_2SO_4 solution (with scan rates varying from 20 to 500 mV s^{-1}). Figure 2(b) shows cyclic voltammograms for a Pd-Pt-PbO_x/C catalyst. These data were taken in the same $Fe(CN)_6^{3-}/Fe(CN)_6^{4-}$ + 0.5 mol L^{-1} H_2SO_4 solution as the Pt electrode. Scan rates were varied from 10 to 250 mV s^{-1}. Calculations of electrochemical active areas for all materials were carried out using the curve at 50 mV s^{-1}.

Table 1. Approximate electrochemical active area calculated for the carbon supported catalysts. All measurements were carried out with a scan rate of 50 mV s^{-1}. The geometric area of the glassy carbon electrode used as support for all catalysts was 0.031 cm^2.

	Pd/C	**Pd-Pt/C**	**Pd-Pt-PbO$_x$/C**
Current of Peak of Oxidation (A) *at 50 mV s^{-1} of scan rate	3.94×10^{-4}	4.33×10^{-4}	4.66×10^{-4}
Approximate Actice Area (cm^2)	0.376	0.413	0.445
Roughness Factor	12.13	13.33	14.35

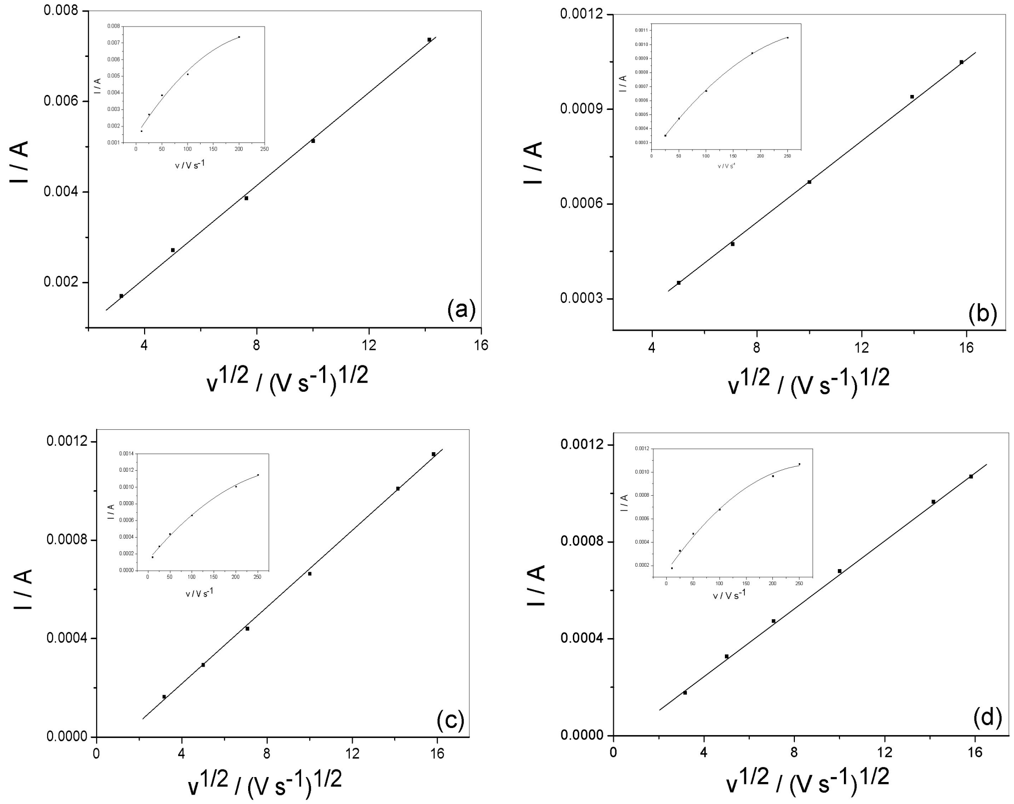

Figure 3. Dependence of the peak of current on the square root of the scan rate for Pt (a), Pd/C (b), Pd-Pt/C (c) and Pd-Pt-PbO$_x$/C (d). The insets show the dependences of the current peaks on the absolute values of the scan rates.

In Figure 2, the concentrated solution was used because returned more linear results. The dotted line (Fig. 2(a)) represents the baseline, and *ΔI* represent the current variation after baseline subtraction. Fig. 2(b) shows a sample calculation of the electrochemical area for a Pd-Pt-PbO$_x$/C catalyst. Curves “a” through “f” (varying in scan rate from 10 to 250 mV s^{-1}) represent the electrochemical responses of the Pd-Pt-PbO$_x$/C catalyst in the reference solution. When determining the electrochemical area, all calculations used data taken at a scan rate of 50 mV s^{-1}. The well-characterized Pt electrode was used as comparison. The electrochemical area for all materials studied can be found in Table 1. These values were used to normalize the currents of the experiments presented in Figures 4 and 5.

Figure 3 shows graphs of current *vs.* scan rate, showing the linear response of the currents as a function of the square root of the scan rate. The insets present a non-linear profile, so the currents are shown as a function of the absolute scan rate. Based on these data, the validity of the comparison between the polycrystalline Pt and the Pd-based catalysts supported in carbon powder is confirmed.

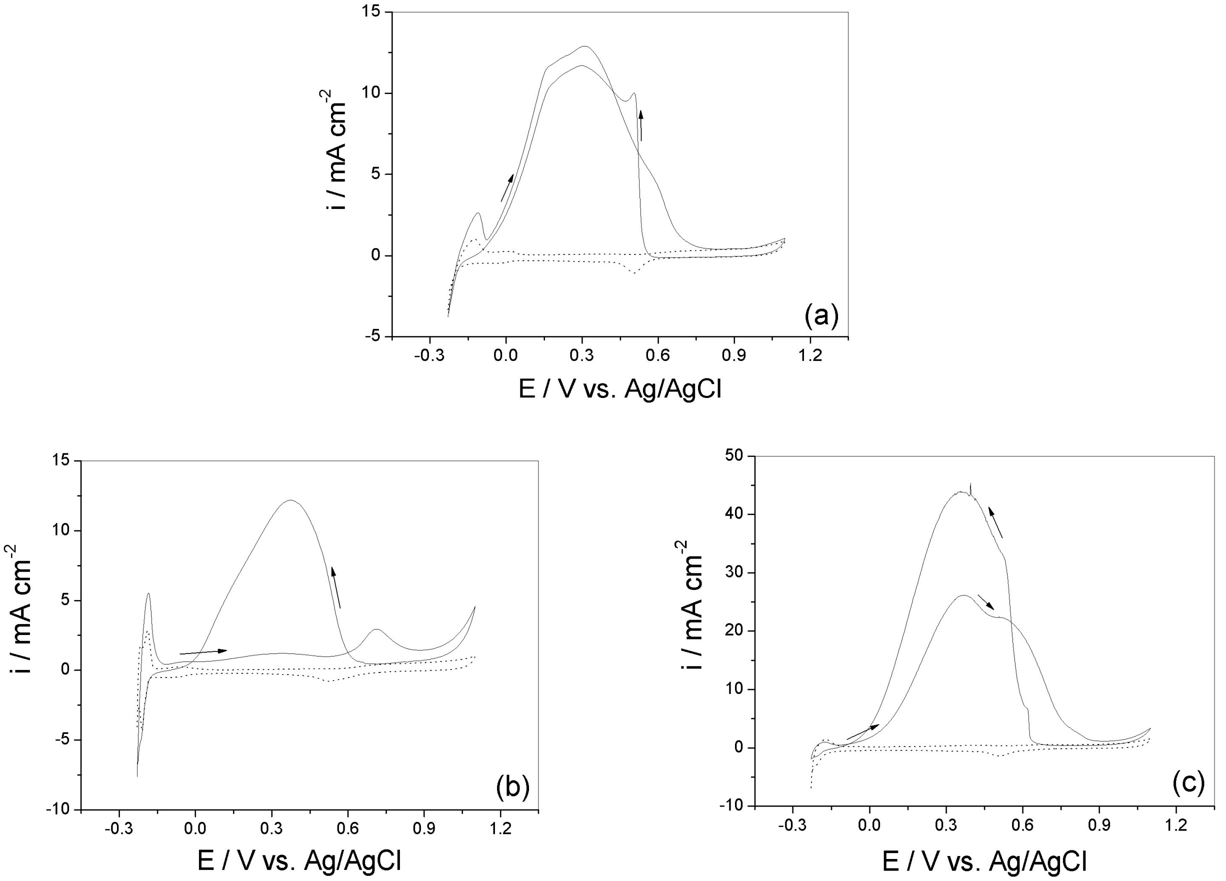

Figure 4. Cyclic voltammograms (CV´s) for Pd/C (a) Pd-Pt/C (b) and Pd-Pt-PbO$_x$/C (c) electrodes in the presence of 1.0 mol L^{-1} formic acid (HCOOH) + 0.5 mol L^{-1} H_2SO_4 solution. The dotted lines represent the electrochemical response of these electrodes in presence of 0.5 mol L^{-1} H_2SO_4. In each case the scan rate was 20 mV s^{-1}.

The electrochemical areas are calculated according to the Randles-Sevcik equation as presented below:

$$i_{peak} = (2.68x10^5)n^{3/2}v^{1/2}AD^{1/2}C^* \quad \text{(eq. 6)}$$

where $i_{(peak)}$ is the peak current density, n is the number of electrons involved in the reaction, v is the scan rate, A is the active area, D is the diffusion coefficient and C^* is the bulk concentration of the studied solution. It is important to observe that the electrochemical area as calculated here must be considered only an approximation, due to the nature of the electrodes analyzed and the concentration of the species in solution. For example, a carbon supported catalyst is porous and has an important roughness factor, which could introduce errors due to different diffusion gradients on the surface of the electrode. Also, the Randles-Sevcik equation is adequate to be used for diluted solutions. Nevertheless, a very good linearity was observed for all studied system.

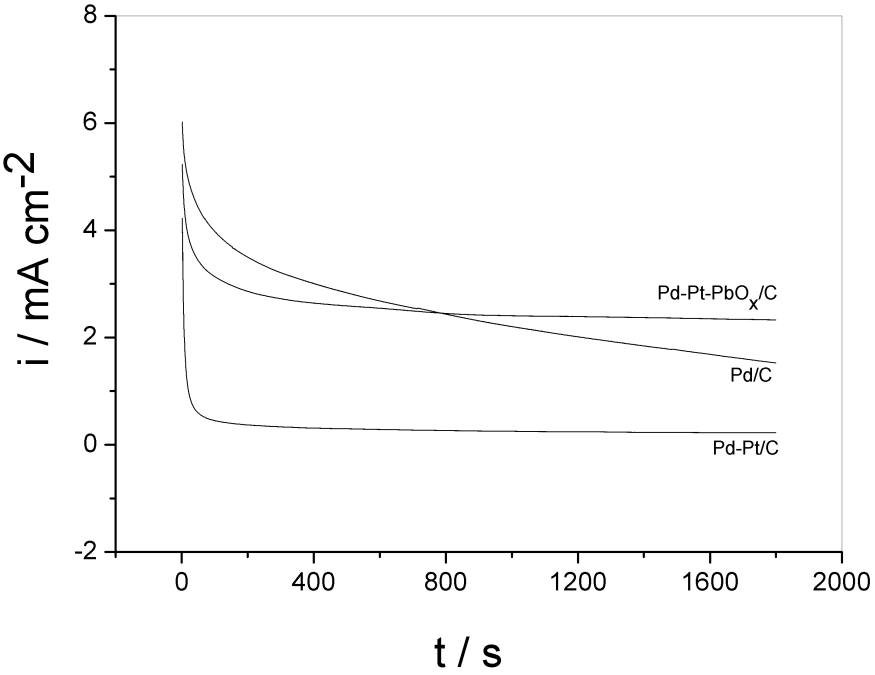

Figure 5. Short current-time responses (at 0.15 V vs. Ag/AgCl) carried out in 1.0 mol L^{-1} formic acid (HCOOH) + 0.5 mol L^{-1} H_2SO_4 solution for Pd/C, Pt-Pd/C and Pd-Pt-PbO_x/C electrodes. The Pd-Pt-PbO_x/C catalyst suffered a very low poisoning process at the beginning of the oxidation. On the contrary, the Pd/C showed slow and continuous current decay during the oxidation process.

The Eq. 6 equation can be better rewritten as:

$$i_{peak} \propto kv^{1/2}A \qquad \text{(eq. 7)}$$

where “k” is a constant.

Electrode areas calculated by this approach are potentially more realistic than those calculated by the CO stripping technique [17] because Pd-based catalysts have no affinity with carbon monoxide.

Fig. 4 shows voltammetric responses of all catalysts studied, both in the presence (full lines) and absence (dotted lines) of formic acid (1.0 mol L^{-1} of HCOOH in H_2SO_4 0.5 mol L^{-1}). For the Pd/C catalyst (a), the profile indicates that the reaction most likely follows the direct pathway due to an inhibited reactivation process in the returning of the scan. This kind of observation of the reaction mechanism of Pd has been observed previously and discussed in recent papers [15, 16]. On the other hand, the Pd-Pt/C catalyst (b) probably follows the indirect pathway, as do the pure Pt electrodes. It is also possible to see in Fig. 4(b) that the oxidation process starts at a very high potential (about 0.7 V vs. Ag/AgCl), enabling important reactivation current in the return of the voltammetric cycle. Finally, the Pd-Pt-PbO_x/C catalyst (c) seems to follow a more pronounced mixture of both direct and indirect mechanisms. For the Pd/C and Pd-Pt-PbO_x/C catalysts, the reaction starts at a very low potential, about 0 V vs. Ag/AgCl. To verify these affirmations, a mechanistic study must be carrying out to elucidate the reaction mechanisms for each catalyst.

The electrochemical behaviour of all electrodes for a fixed polarization potential were studied briefly at 0.15 V vs. Ag/AgCl. The performance of the Pd-Pt/C catalyst was not satisfactory at this fixed potential of 0.15 V vs. Ag/AgCl. This effect is probably related to separation of the Pt and Pd phases. As previously commented, Waszczuk et al. [12] showed that Pt-Pd catalysts performed best compared with pure Pt and Pt-Pd-Ru catalysts, but, in this case, all materials formed well-defined alloys.

In contrast, the behaviour of the Pd-Pt-PbO_x/C catalyst was interesting due to the presence of a small amount of poisoning during the process, especially when compared with the Pd/C catalyst. As previously commented, slow and continuous decay is commonly observed in current vs. time experiments of oxidation of this acid for Pd-based electrodes, due to the presence of poisoning agents such as formate [13], sulphate [14] or other anions [15]. The Pd-Pt-PbO_x/C catalyst is less susceptible to this kind of poisoning, compared with the Pd/C catalyst.

4. CONCLUSIONS

A polycrystalline Pt electrode and a solution of $Fe(CN)_6^{3-}/Fe(CN)_6^{4-}$ can be used as references to calculate approximate electrochemical active areas for several kinds of electrode materials. For all catalysts, the roughness factor varied from about 12.0 to 15.5. This sort of calculation is most useful for materials that do not have any affinity towards CO, which renders invalid the calculation by using a more standard carbon monoxide desorption technique. Electrochemical studies revealed that the Pd-Pt-PbO_x/C catalyst had the best catalytic performance compared with Pd-Pt/C and Pd/C materials, mainly due to the low capacity of absorption of poisoning agents such as sulphate.

ACKNOWLEDGEMENTS
We thank the Brazilian agencies FAPESP (2007/05155-1), CNPq (472476/2008-4 and 301863/2008-3), CAPES and UFABC-PRPG for providing G.S. Buzzo and R.V. Niquirilo with scholarships. ETN thank Prof. Vera R.L. Constantino from IQ-USP for use of the XRD instrument.

References

1. X. Yu and P.G. Pickup, *Electrochem. Comm*, 11 (2009) 2012.
2. Y. Suo and I-Ming Hsing, *Electrochim. Acta*, 55 (2009) 210.
3. Y. Wang, B. Wu, Y. Gao, Y. Tang, T. Lu, W. Xing and C. Liu, *J. Power Sources*, 192 (2009) 372.
4. Xiao-Ming Wang and Yong-Yao Xia, *Electrochim. Acta*, 54 (2009) 7525.
5. C. Hartnig, J. Grimminger and E. Spohr, *J. Electroanal. Chem.* 607 (2007) 133.
6. R. Wang, S. Liao and S. Ji, *J. Power Sources* 180 (2008) 205.
7. J. Wang, G. Yin, Y. Chen, R. Li and X. Sun, *Int. J. Hydrogen Energy*, 34 (2009) 8270.
8. D. Morales-Acosta, J. Ledesma-Garcia, L. A. Godinez, H. G. Rodríguez, L. Álvarez-Contreras and L. G. Arriaga, *J. Power Sources* 195 (2010) 461.
9. S. Ha, R. Larsen and R.I. Masel, *J. Power Sources* 144 (2005) 28.
10. R. Larsen, J. Zakzeski and R I. Masel, *J. Electrochem. Solid-State Lett.* 8 (2005) 291.
11. Y.M Zhu, Z. Khan and R.I. Masel, *J. Power Sources* 139 (2005) 15.
12. P. Waszczuk, T.M. Barnard, C. Rice, R.I. Masel and A. Wieckowski, *Electrochem. Comm.* 4 (2002) 599.
13. W.P. Zhou, A. Lewera, R. Larsen, R.I. Masel, P.S. Bagus and A. Wieckowski, *J. Phys. Chem. B* 110 (2006) 13393.
14. F.J. Vidal-Iglesias, J. Solla-Gullon, E. Herrero, A. Aldaz and J.M. Feliu, *J. Appl. Electrochem.* 36 (2006) 1207.
15. M. Arenz, V. Stamenkovic, T.J. Schmidt, K. Wandelt, P.N. Ross and N.M. Markovic, *Phys. Chem. Chem. Phys.* 5 (2003) 4242.
16. X. Yu and P.G. Pickup*, Electrochem. Commun*. 11 (2009) 2012
17. L.P.R. Profeti, D. Profeti and P. Olivi, *Int. J. Hyd. Energy,* 34 (2009) 2747
18. J. Ribeiro, D. M. dos Anjos, K. B. Kokoh, C. Coutanceau, J.-M. Léger, P. Olivi, A. R. de Andrade and G. Tremiliosi-Filho, *Electrochim. Acta* 52 (2007) 6997.
19. P. Kim, J.B. Joo, W. Kim, J. Kim, I. K. Song and J. Yi, *J. Molecular Cat. A: Chemical* 263 (2007) 15.
20. N. de-los-Santos-Álvarez, L.R. Alden, E. Rus, H. Wang, F.J. DiSalvo and H.D. Abruña, *J. Electroanal. Chem.* 626 (2009) 14
21. J. Jin, M. Prochaska, D. Rochefort, D. K. Kim, L. Zhuang, F. J. DiSalvo, R. B. van Dover and H.D. Abruña, *App. Surf. Sci.* 254 (2007) 653.
22. S.P.E. Smith and H.D. Abruña, *J. Electroanal. Chem.* 467 (1999) 43.
23. H.B. Suffredini, G.R. Salazar-Banda and L.A. Avaca, *J. Sol Gel Sci. Tech.* 49 (2009) 131.
24. H.B. Suffredini, G.R. Salazar-Banda and L.A. Avaca, *J. Power Sources* 171 (2007)355.
25. Chung-Kwei Lin, Kai-Han Chuang, Chia-Yen Lin, Chien-Yie Tsay and Chin-Yi Chen, *Surf. Coat. Tech.* 202 (2007) 1272.
26. C. Guo, F. Gao, L. Liang, B. C. Choi and Jung-Hyun Jeong, *J. Alloys and Compounds*, 479 (2009) 607.
27. T. P. Ang, *Catalysis Comm.*, 10 (2009) 1920

© 2010 by ESG (www.electrochemsci.org)